Heliyon 10 (2024) e30902

Contents lists available at ScienceDirect

Heliyon

journal homepage: www.cell.com/heliyon

Research article

Hydrogen therapy promotes macrophage polarization to the M2 subtype in radiation lung injury by inhibiting the NF-κB signalling pathway

Xue Gao [a,b], Shiying Niu [a,c], Lulu Li [a], Xiaoyue Zhang [b], Xuetao Cao [a], Xinhui Zhang [a,b], Wentao Pan [a], Meili Sun [c,d], Guoli Zhao [e], Xuezhen Zheng [a,b], Guohua Song [a,**], Yueying Zhang [a,b,*]

[a] Department of Pathophysiology, School of Clinical and Basic Medicine, Shandong First Medical University, China
[b] Department of Pathology, The First Affiliated Hospital of Shandong First Medical University, China
[c] Department of Pathology, Linfen Central Hospital, China
[d] Department of Oncology, Affiliated Central Hospital of Shandong First Medical University, China
[e] Department of Pathology, Liaocheng Infectious Disease Hospital, China

ARTICLE INFO

Keywords:
Hydrogen
Radiation lung injury
Macrophage polarization
Toxic injury
Pathological mechanism

ABSTRACT

Background: Radiotherapy has become a standard treatment for chest tumors, but a common complication of radiotherapy is radiation lung injury. Currently, there is still a lack of effective treatment for radiation lung injury.

Methods: A mouse model of radioactive lung injury (RILI) was constructed and then treated with different cycles of hydrogen inhalation. Lung function tests were performed to detect changes in lung function.HE staining was used to detect pathological changes in lung tissue. Immunofluorescence staining was used to detect the polarization of macrophages in lung tissue. Immunohistochemistry was used to detect changes in cytokine expression in lung tissues. Western Blot was used to detect the expression of proteins related to the NF-κB signalling pathway.

Results: Lung function test results showed that lung function decreased in the model group and improved in the treatment group.HE staining showed that inflammatory response was evident in the model group and decreased in the treatment group. Immunohistochemistry results showed that the expression of pro-inflammatory factors was significantly higher in the model group, and the expression of pro-inflammatory factors was significantly higher in the treatment group. The expression of pro-inflammatory factors in the treatment group was significantly lower than that in the model group, and the expression of anti-inflammatory factors in the treatment group was higher than that in the model group. Immunofluorescence showed that the expression of M1 subtype macrophages was up-regulated in the model group and down-regulated in the treatment group. The expression of M2 subtype macrophages was up-regulated in the treatment group relative to the model group. Western Blot showed that P–NF-κB p65/NF-κB p65 was significantly increased in the model group, and P–NF-κB p65/NF-κB p65 was decreased in the treatment group.

* Corresponding author. Tumor Pathology, Department of Pathophysiology, School of Clinical and Basic Medicine, Shandong First Medical University & Shandong Academy of Medical Sciences, China.
** Corresponding author. Department of Pathophysiology, School of Clinical and Basic Medical Sciences, Shandong First Medical University & Shandong Academy of Medical Sciences, China.

https://doi.org/10.1016/j.heliyon.2024.e30902
Received 14 January 2024; Received in revised form 4 May 2024; Accepted 7 May 2024
Available online 11 May 2024

Conclusion: Hydrogen therapy promotes macrophage polarization from M1 to M2 subtypes by inhibiting the NF-κB signalling pathway, thereby attenuating the inflammatory response to radiation lung injury.

1. Introduction

Radiation therapy has become a standard treatment in the clinical management of thoracic tumors, but radiotherapy can inevitably lead to radiation lung injury (RILI) [1,2]. Macrophages are essential cells in the inflammatory response in the body. When stimulated, macrophages undergo different differentiation in function and phenotype, called macrophage polarization. When radiation lung injury occurs in the body, macrophages are usually polarised towards the M1 subtype and secrete pro-inflammatory factors such as tumour necrosis factor-alpha (TNF-α) and interleukin 6 (IL-6) [3,4]. These pro-inflammatory factors induce the activation of M2 subtype macrophages, which inhibit the inflammatory response and promote the role of tissue repair, express CD206, and produce anti-inflammatory factors such as interleukin 10 (IL-10). Mild inflammatory reactions in lung tissue can dissipate on their own. In contrast, severe inflammatory responses may lead to extensive lung fibrosis; therefore, radiation lung injury requires prompt treatment [5].

There are more significant difficulties in treating RILI, and there is currently no U.S. Food and Drug Administration-approved treatment for RILI. The drugs used in the clinic to treat radiological lung injury are mainly hormonal [1,6], and the commonly used drugs include prednisone. Cases confirm that azathioprine and cyclosporine can treat radiological lung injury [7,8]. Amifostine is the only radioprotective agent currently approved for clinical use. However, these drugs have many side effects and adverse reactions. Relapse is possible following a response to hormones; Amifostine causes low blood pressure and severe nausea in patients. The above drugs do not fully meet the clinical needs. Many studies have confirmed that hydrogen is an inflammation inhibitor and that the intake of hydrogen molecules through various routes can significantly inhibit the inflammation response [9–11]. The exact mechanism still needs to be elucidated. Therefore there is an urgent need to investigate the specific therapeutic mechanism of hydrogen in RILI and to find an effective hydrogen treatment for RILI [12,13].

In this study, we established an animal model of radiation lung injury in mice. We administered different cycles of hydrogen inhalation to investigate the role of hydrogen in reducing radiation lung injury and the specific mechanism from the perspective of macrophage polarization.

2. Material and methods

2.1. Animal

A total of 40 healthy C57BL/6 mice with a weight of 18–22 g and an age of approximately 8 weeks were purchased from the Jinan Pengyue Experimental Animal Technology Co. All animals were housed under standard conditions (22 ± 2 °C, 55 ± 10 % humidity, 12 h light/dark cycle) with free access to standard mouse chow and water. Forty C57BL/6 mice were randomly divided into 4 groups, including the control group (no irradiation), model group (irradiation group only), the hydrogen treatment group 1(irradiation followed by 2 weeks of hydrogen inhalation treatment), and the hydrogen treatment group 2 (irradiation followed by 5 weeks of hydrogen inhalation treatment). All mice were necropsied after anesthesia in the fifth week after the experiment, and the lung tissues were quickly removed. The left lung was snap frozen and stored for protein immunoblotting (Western blot); the right lung was fixed in 10 % formaldehyde solution and used for routine pathology, immunofluorescence, and immunohistochemistry. All animal experiments were approved by the Experimental Animal Ethics Committee of Shandong First Medical University (W202311160312). All methods were performed in accordance with the relevant guidelines and regulations.

2.2. Irradiation

The modelling method of radiation lung injury used in this study is based on the previously published literature of our research group.In the preliminary experiments of our group, C57BL/6J mice were used as irradiation carriers, and different irradiation doses of 0Gy, 8Gy, 12Gy, 16Gy and 20Gy were used to establish a mouse model of RILI, and mice were dissected 5w, 6w and 7w after irradiation, respectively. Based on the pathological changes in the lung tissue, we finally used an irradiation dose of 20 Gy to establish a mouse model of RILI and dissected the mice 5 weeks after irradiation [14].Mice were irradiated at Jinan Central Hospital Radiotherapy Department. Before irradiation, mice were anesthetized by intraperitoneal injection of 2 % pentobarbital and placed on an irradiation table with the thorax exposed to the irradiated area. All mice were arranged in rows, and the thorax was irradiated according to the grouping requirements. X-rays of 6 MV were used at a dose rate of 2 Gy/min. The total dose to the lung tissue was 20 Gy. Control mice were left untreated.

2.3. Intervention with hydrogen

Animals were treated with 4 % hydrogen inhalation for 4 h at the same time each day after irradiation using a homemade hydrogen delivery device [13]. Hydrogen and air were supplied by a hydrogen generator (SPE-300, Jinan Haowei Experimental Instruments Co.,

Ltd.) and an air generator (LCA-3, Shanghai Bonsey Instruments Technology Co., Ltd.), respectively, and the flow rate was adjusted by a gas flow meter so that the volume fraction of mixed hydrogen was 4 %. The total gas flow rate was approximately 3 L/min. The hydrogen concentration was confirmed using a hydrogen detector (XP-3140, New Cosmos, Japan).

2.4. Lung function

The EMKA lung function analysis system (EMKA,Montrichard-Val-de-Cher, France) was used to detect the lung function of mice. Unconstrained whole-body volume tracing (WBP) has been used to detect changes in lung function in mice. The non-invasive whole-body plethysmography (WBP) is a state-of-the-art device for measuring respiratory physiological indices and evaluating bronchoconstriction and other parameters in awake and free-ranging animals. Working Principle:Animals in the body plethysmograph, due to the respiratory rhythm, produce pressure changes when the animal breathes: when air enters the animal from the room, → the pressure of the box decreases (nasal airflow), the chest expands →, the pressure of the box rises (thoracic airflow) → the sensor detects the combination of these two effects. (1) The sensor outside the body plethysmograph is connected to the body plethysmograph and the mice are placed in a stable condition inside the closed body plethysmograph to start the test. (2) The chamber volume changes as the animal's thorax undulates, which is converted into an electrical signal by an amplifier and pressure transducer, then processed by the computer, which displays the respiratory curve. (3) The software processes the curve to calculate peak inspiratory flow, expiratory flow, tidal volume and respiratory parameters.

2.5. Hematoxylin-eosin (H&E) staining

The tissue on the sections was stained using H&E staining and analysed for structural and morphological features, such as the degree of structural disruption and the extent of inflammatory cell infiltration. Tissue changes were observed using a light microscope (Leica, Wetzlar, Germany). For these analyses, stained sections were observed using a 3D scanner (3DHISTECH, Budapest, Hungary).

2.6. Immunofluorescence

(1) The paraffin-embedded blocks containing tissues were sliced on a slicer with a slice thickness of 4 μm. (2) The prepared slices were baked on a baking machine for 1h to melt the paraffin wax on the tissues; then the slices were sequentially put into two vats of xylene to be dewaxed again; after dewaxing, they were immersed in an alcohol solution with concentrations ranging from high to low, and finally put into double-distilled water. (3) A 3 % H_2O_2 solution (1.5 ml of 30 % H_2O_2 solution + 500 ml of distilled water) was prepared, and the reaction was carried out under light for 20 min to eliminate endogenous peroxidase activity. After completion, the sections were washed with distilled water for 5min × 2 times. (4) To expose the antigenic determinant clusters for better binding with antibodies, the sections were placed in a pre-prepared citric acid repair solution, boiled at 100 °C for 20min, and left to cool naturally to room temperature. Sections were taken out and washed using PBS for 5min × 3 times.(5) PBS was blotted around the tissues with absorbent paper, and the sections were blocked in PBS containing 5 % goat serum at 37 °C for 1 h (6) PBS diluted primary antibody CD206 (bsm-60761R, Bioss, China) ratio 1:300, CD86 (bsm-1035R, Bioss, China) ratio 1:300 and F/480 (bsm-34028 M, Bioss, China) 1:300 were added dropwise, and the sections were incubated in the refrigerator at 4 °C overnight. (7) On the next day, the sections were taken out from the refrigerator, and after the sections were returned to room temperature, they were washed in PBS for 5 min × 3 times. (8) The sections with primary antibodies of CD86 and CD206 were added with fluorescent secondary antibody dilution of goat anti-rabbit (1:100); the sections with primary antibody of F/480 were added with fluorescent secondary antibody dilution of goat anti-mouse (1:300). (9) Incubate at 37 °C away from light for 1h, wash with PBS for 5min × 3 times, and then dropwise seal the sections with DAPI-containing anti-quenching sealer. (10) A 3D scanner (3DHISTECH, Budapest, Hungary) was used for film scanning and analysis. The CD86/CD206 fluorescence levels in the tissues were quantified using the Image J software and normalized to the levels of DAPI.

2.7. Immunohistochemistry

(1) The paraffin-embedded blocks containing tissues were sliced on a slicer with a slice thickness of 4 μm. (2) The prepared slices were baked on a baking machine for 1h to melt the paraffin wax on the tissues; then the slices were sequentially put into two vats of xylene to be dewaxed again; after dewaxing, they were immersed in an alcohol solution with concentrations ranging from high to low, and finally put into double-distilled water. (3) A 3 % H_2O_2 solution (1.5 ml of 30 % H_2O_2 solution + 500 ml of distilled water) was prepared, and the reaction was carried out under light for 20 min to eliminate endogenous peroxidase activity. After completion, the sections were washed with distilled water for 5min × 2 times. (4) To expose the antigenic determinant clusters for better binding with antibodies, the sections were placed in a pre-prepared citric acid repair solution, boiled at 100 °C for 20min, and left to cool naturally to room temperature. Sections were taken out and washed using PBS for 5min × 3 times. (5) PBS was blotted around the tissues with absorbent paper, and the sections were blocked in PBS containing 5 % goat serum at 37 °C for 1 h .(6) Dropwise add PBS diluted primary antibody IL-6 (bs-0782R, Bioss, China) ratio 1:300, TNF-α (bs-10802R, Bioss, China) ratio 1:300, and IL-10 (bs-6761R, Bioss, China) 1:300, and incubate at 4 °C in the refrigerator overnight. (7) On the next day, the sections were removed from the refrigerator and washed with PBS for 5 min × 3 times after the section temperature was returned to room temperature. (8) Add HRP-labelled goat anti-rabbit secondary antibody (1:200) dropwise on the sections, incubate for 1h at 37 °C in an incubator, and wash with PBS for 5min × 3 times. (9) Prepare 3,3-diaminobenzimidazole (DAB) chromogenic solution (substrate solution: concentrate solution = 1000:50),

mix well, add the DAB chromogenic solution dropwise onto the tissue, wait for 3–5min, and observe the colour development under the microscope; at the end of the chromogenic development, stain the nuclei of the cells with hematoxylin for 2min. (10) Immerse the sections into the alcoholic solution with the concentration ranging from low to high, and finally put into the xylene I, Xylene II for 10min each, neutral gum sealing, and observe the staining under the light microscope. (11) Sections were scanned and analysed using a 3D scanner (3DHISTECH, Budapest, Hungary). (12)Staining score was determined as 0: 0–5% of staining cells, 1: 6–25 % of staining cells, 2: 26–50 % of staining cells, 3: 51–75 % of staining cells, and 4: >75 % of staining cells. Staining intensity was scored as 0–1: negative, 2–3: weak positive, 4–5: intermediate, and 6–7: strong positive. The sum of both extent and intensity score was defined as the staining final score [15].

2.8. Western blotting analysis

(1) Steps for extracting lung tissue proteins: All operations were performed on ice. Weigh about 50–100 mg of fresh lung tissue in a centrifuge tube, add pre-cooled saline, and shake the tissue up and down with tweezers to remove the blood on the surface of the lung tissue. The tissue was put into 500-1000μl of protein lysate (RIPA lysate: protease inhibitor PMSF = 100:1) prepared in advance. It was broken at high speed on a tissue homogeniser for 2 min at 60HZ, and then the shocked tissue was put into a coagulator and mixed up and down for 15 min so as to make it sufficiently lysed. The tissue was centrifuged at a low temperature of 4 °C and 12000r for 15 min, and the supernatant was aspirated into a new centrifuge tube. The supernatant was transferred to a new centrifuge tube, and protein gel electrophoresis buffer was added, mixed well, and then boiled in water at 100 °C for 10 min. After cooling, it was stored at −20 °C for short-term storage and at −80 °C for long-term storage for the next step of the experiments. (2) Rinse the gel plate with single-distilled and double-distilled water, and dry it for spare. (3) The prepared lower layer of gel (8 % separator gel) was quickly filled into the gel plate, and the lower layer of gel was solidified after about 1h at room temperature; the prepared upper layer of gel (concentrated gel) was quickly filled into the gel plate, and it was left at room temperature for 30min. (4) After the solidification of the upper layer of concentrated gel, put the gel plate into the electrophoresis tank, fix it with a clamp, fill up the tank with electrophoresis solution, and use a pipette gun to sample the samples with 30 μg/well aliquot. The marker volume of sampling is 2.5 μl (5) Carry out electrophoresis, at first constant voltage 80V electrophoresis, about 40 min later, using 150V in the lower layer of gel electrophoresis. (6) Half an hour before transferring the membrane, place the transfer solution at −20 °C for pre-cooling. Cut the PVDF membrane according to the size of the electrophoretic adhesive, soak the PVDF membrane in methanol for 60 s, and mark the PVDF membrane by cutting the corners. Assemble the transfer clamps according to the way of black side-sponge-filter paper-electrophoresis adhesive-PVDF membrane-filter paper-sponge-transparent side. Add the membrane transfer clips and membrane transfer solution into the membrane transfer tank. The membrane was transferred in constant pressure mode, 100 V, 90 min (7) The transferred PVDF membrane was washed with TBST solution to remove the surface transfer solution. Subsequently, it was placed in 5 % closed milk for 90 min. At the end of the closure, the membrane was rinsed with TBST solution for 5 min × 3 times. (8) Primary antibodies were diluted with primary antibody diluent: β-actin (66009-1-Ig, Proteintech, China) at 1:20,000, NF-κB p65 (66535-1-Ig, Proteintech, China) at 1:2,000, and Phospho-NFκB p65 (bs- 3485R, Bioss, China) at 1:200. The bands were cut according to the molecular weight of the proteins and placed in the diluted primary antibody solution respectively, and incubated in the refrigerator at 4 °C overnight. (9) After the primary antibody incubation, rinsed using TBST solution for 5 min × 3 times. The bands of primary antibody for β-actin and NF-κB p65 were added to the secondary antibody dilution of goat anti-rabbit (SA00001-2, Proteintech, China) 1:5000. The bands of primary antibody for Phospho-NFκB p65 were added to the secondary antibody dilution of goat anti-mouse (SA00001-1, Proteintech, China) 1:5000 secondary antibody dilution. The strips were incubated in the secondary antibody dilution at room temperature for 1 h (10) At the end of the secondary antibody incubation, the strips were rinsed in TBST for 5 min × 3 times. The protein bands were observed using ECL reagents (Millipore, USA). (11)The ratios of the protein band intensities relative to that of β-Actin were calculated for each sample using Image J.

2.9. Statistical analysis

Plotted and analysed using GraphPad Prism 8.0.1 software, and the measurement data were expressed as mean ± standard deviation. Comparisons between multiple data groups were made by one-way classification ANOVA analysis, and comparisons between two groups were made using the two independent samples *t*-test, with $P < 0.05$ indicating that the differences were statistically significant. Three biological replicates were performed for each experiment.

3. Results

3.1. Hydrogen therapy improves lung function in mice with radiation-induced lung injury

We investigated the changes in pulmonary ventilatory function in mice after 5 weeks of radiation injury to test whether our modelling was successful and whether hydrogen improves lung function in mice.Lung function in mice was assessed using the EMKA lung function analysis system (EMKA). The primary lung function indicators include (1) lung volume index: tidal volume (TVb), the volume of inhaled or exhaled gas during each breath. (2) Conductivity index: peak inspiratory flow (PIF), peak flow rate during inspiration; peak expiratory flow (PEF), peak flow rate during expiration. (3) Airway obstruction index: expiratory flow 50 (EF50), indicates the expiratory flow rate at 50 % of the exhaled tidal volume. (4) Ventilation index: minute volume (MVb), the total amount of gas inhaled or exhaled per minute.The results showed that compared with the control group, the lung function of mice in the model

group decreased, and TVb, MVb, PIFb, PEFb, and EF50 were all significantly lower; the lung function of mice in the treatment group improved, and TVb, MVb, PIFb, PEFb, and EF50 were all higher; and the effect of the treatment group 2 was better than that of the treatment group 1. Because the mice's activity and mood affected the pulmonary function tests, there was a large bias in the pulmonary function tests. Treatment group 1 showed a trend of remission relative to the model group, but it was not statistically significant, and the recovery of the mice's pulmonary function might be delayed relative to the pathological changes.These results indicate that hydrogen can significantly improve lung function in mice (Table 1).

3.2. Hydrogen therapy alleviated pathological changes in lung tissue in mice with radiation lung injury

The pathology of radiation lung injury is characterised by diffuse alveolitis, pathological proliferation of fibroblasts, and deposition of extracellular matrix in the interstitium and alveolar spaces. As demonstrated in previous experiments, inflammatory cell infiltration, alveolar septal thickening, and capillary congestion were observed in the lung tissue of C57BL/6 mice after X-ray irradiation [14]. Histopathological changes in the lungs of the mice were observed using HE staining. The results showed that the model group (Fig. 1B) had thickened alveolar septum, edema, dilated and congested blood vessels, and infiltrated inflammatory cells compared to the control group(Fig. 1A). The above results demonstrate that we successfully constructed a mouse model of radiological lung injury. In contrast, the lesions in the hydrogen treatment group (Fig. 1C–D)were significantly less than those in the model group, and the inflammatory response was attenuated.

3.3. Hydrogen therapy can significantly promote macrophage polarization from the M1 subtype to the M2 subtype

Mouse-derived F4/80 is mainly expressed on the surface of macrophages and is used as a marker of mature macrophage tissue [16]. In this experiment, F4/80 was labelled with green fluorescence; activated M1 macrophages expressed cluster of differentiation 86 (CD86) on their membrane surface, and CD86 was labelled with red fluorescence in this experiment [17]. M2 macrophages highly expressed mannose receptor (MR/CD206) [17], and CD206 was fluorescently labelled in red in this experiment.The results showed that the expression of CD86, a molecular marker of the M1 subtype macrophage surface, was significantly increased in the lung tissue of the model group compared with that of the control group(Fig. 2A–B); the expression of CD206, a molecular marker of the M2 subtype macrophage surface, was not significantly increased(Fig. 2C–D). The presentation of CD86, a molecular tag on the surface of M1 subtype macrophages, was significantly reduced in the hydrogen-treated group compared with the model group(Fig. 2A–B). In contrast, the expression of CD206, a molecular marker on the surface of M2 subtype macrophages, was significantly increased in treatment group 2 compared with treatment group 1(Fig. 2C–D). These results indicate that hydrogen can substantially promote the polarization of macrophages from the M1 subtype to the M2 subtype.

3.4. Hydrogen therapy can significantly inhibit the inflammatory response in radiation-induced lung injury

Immunohistochemistry showed that the expressions of inflammatory cytokines IL-6 and TNF-α in the model group were much higher than those in the control group(Fig. 3A–D). The expression of IL-6 and TNF-α was much lower in the treatment group than in the model group(Fig. 3A–D). The expression of IL-10 in the treatment group was higher than in the model group(Fig. 3E–F). These results suggest that during the inflammatory response to radiation lung injury, M1 subtype macrophages may produce inflammatory molecules, including IL-6 and TNF-α. Hydrogen therapy can significantly reduce the expression of these factors, promote the expression of anti-inflammatory factors such as IL-10, and prevent the inflammatory response of radiation lung injury.

3.5. Hydrogen therapy can significantly inhibit the NF-κB signalling pathway of inflammatory response

An NF-κB signalling pathway is a classical anti-inflammatory pathway in which NF-κB, as a nuclear transcription factor, can induce the expression of inflammatory factors in immune cells and is an essential driving factor for the pro-inflammatory function of macrophages, which promotes the polarization of macrophages towards M1 subtype. Inhibition or activation of the NF-κB signalling pathway significantly affects macrophage polarization. We examined the phosphorylation of NF-κB p65, a protein associated with the NF-κB signalling pathway. The results of protein immunoblotting showed that P–NF-κB p65/NF-κB p65 increased significantly in the model group compared with the control group (Fig. 4A–C). Compared with the model group, P–NF-κB p65/NF-κB p65 was reduced considerably in the hydrogen treatment group (Fig. 4A–C). These results suggest that hydrogen therapy can significantly inhibit NF-κB

Table 1
Comparison of lung function parameters of C57BL/6 mice in each group.

Groups	TVb	MVb	PIFb	PEFb	EF50
Control group	0.29 ± 0.02[a]	138.13 ± 17.87[a]	10 ± 0.9*	6.07 ± 0.77[a]	0.4 ± 0.07[a]
Model group	0.24 ± 0.02	107.61 ± 16.3	8.09 ± 0.87	4.95 ± 0.79	0.3 ± 0.06
Treatment group 1	0.25 ± 0.009	117.73 ± 4.17	8.8 ± 0.44	5.6 ± 0.18	0.35 ± 0.02
Treatment group 2	0.27 ± 0.01 [a]	137.72 ± 8.62 [a]	9.33 ± 0.59 [a]	6.2 ± 0.69 [a]	0.42 ± 0.06 [a]

Note.
[a] Compared with Model group, $P < 0.05$.

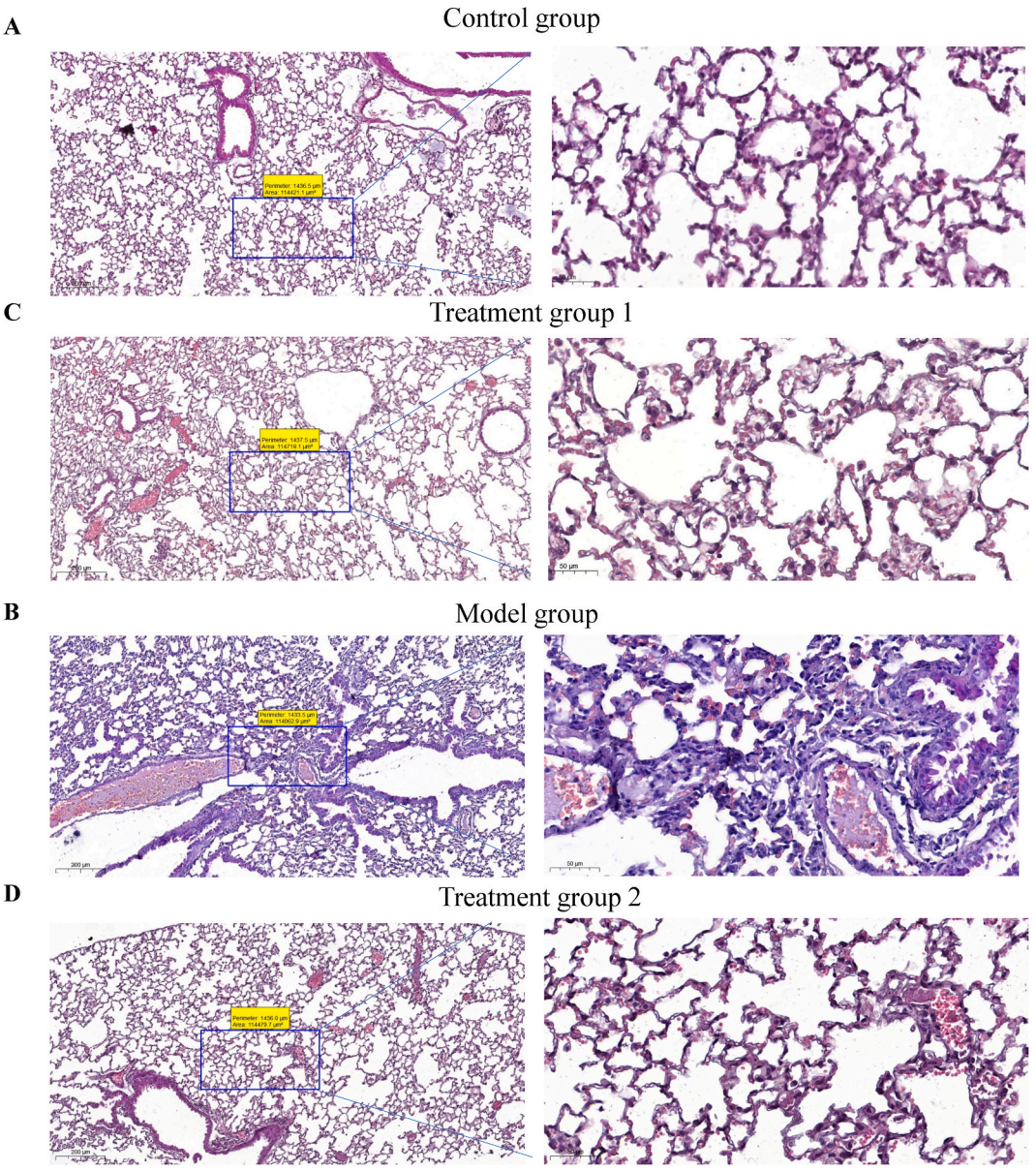

Fig. 1. Hydrogen therapy alleviated pathological changes in lung tissue in mice with radiation lung injury.**A:** HE staining of lung tissue in Control group mice. In the left picture, the scale bar is 200 μm; the right picture is the enlargement of the left picture (in the blue box), the scale bar is 50 μm **B:** HE staining of lung tissue of model group mice. In the left picture, the scale bar is 200 μm; the right picture is a magnification of the local area of the left picture (in the blue box), and the scale bar is 50 μm **C:** HE staining of lung tissue from Treatment group 1 mice. In the left picture, the scale bar is 200 μm; the right picture is a magnification of the local area of the left picture (in the blue box), and the scale bar is 50 μm.**D:** HE staining of lung tissue of Treatment group 2 mice. In the left picture, the scale bar is 200 μm; the right picture is the enlargement of the left picture (in the blue box), the scale bar is 50 μm.

signalling.

4. Discussion

In treating thoracic tumors, radiotherapy has become the primary therapeutic means for treating common thoracic tumors [18]. Radiotherapy often leads to radiation lung injury [1]. The pathological changes of radiation lung injury are mainly inflammatory reactions, manifested by increased inflammatory cells such as monocytes and neutrophils at the injury site and the secretion of many pro-inflammatory factors, IL-6 and TNF-α [19]. Radiation lung injury can lead to radiation-induced fibrosis months to years after initial radiation exposure, closely related to oxidative stress [20]. The two mechanisms of oxidative stress and inflammation interact and

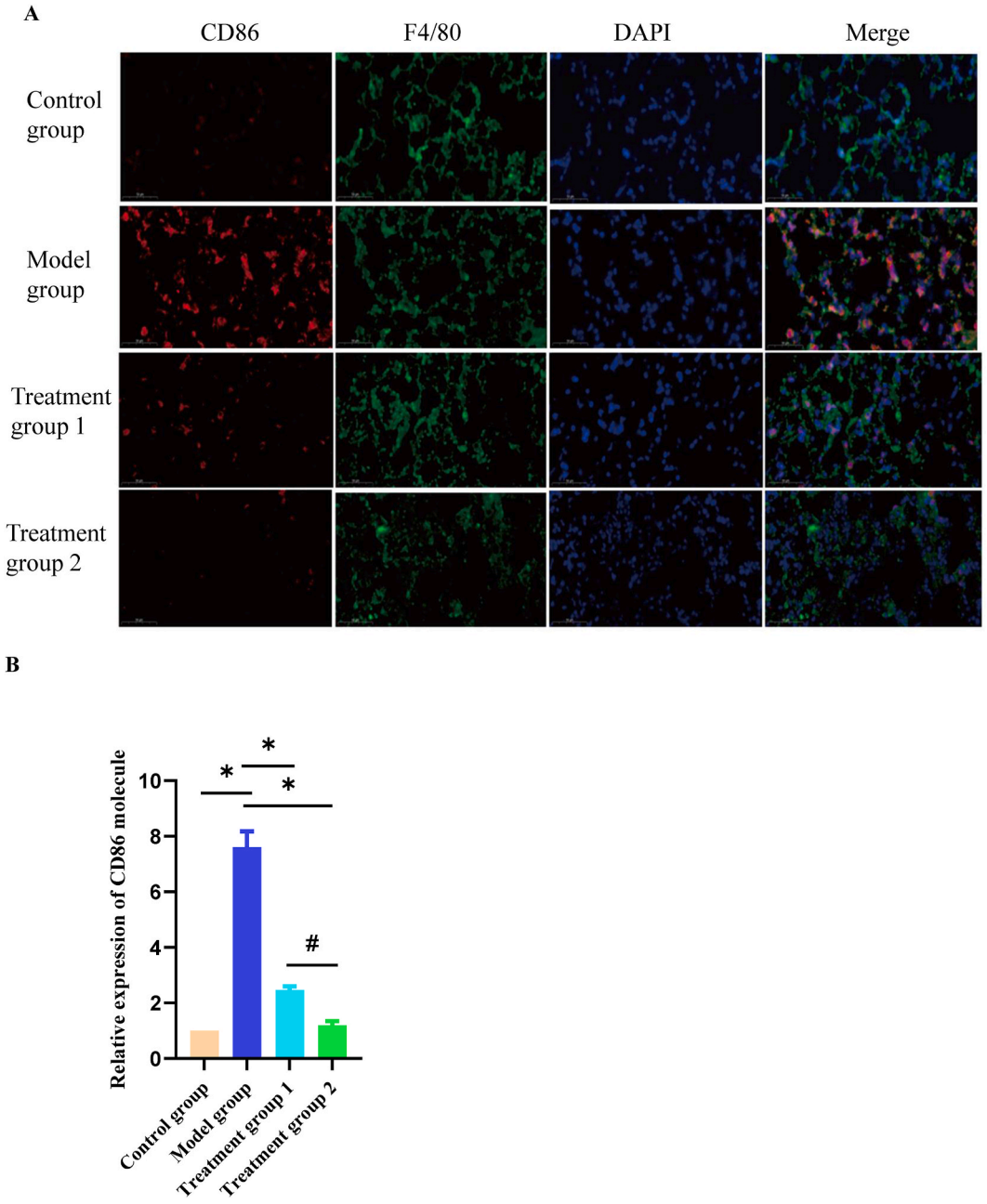

Fig. 2. Hydrogen therapy can significantly promote macrophage polarization from the M1 subtype to the M2 subtype. **A:** Immunofluorescence technique to observe the number of M1 subtype macrophages in mouse lung tissues, scale bar is 50 μm **B:** Histogram of the expression of M1 subtype macrophages in mouse lung tissues detected by immunofluorescence. Data are expressed as mean ± SD, n = 3.* Compared with the model group, $P < 0.05$.# Compared with the treatment group 1, $P < 0.05$.**C:** Immunofluorescence technique to observe the number of M2 subtype macrophages in mouse lung tissues, scale bar is 50 μm.**D:** Histogram of the expression of M2 subtype macrophages in mouse lung tissues detected by immunofluorescence. Data are expressed as mean ± SD, n = 3.* Compared with the model group, $P < 0.05$.# Compared with the treatment group 1, $P < 0.05$.

regulate each other in the progression of radiation lung injury disease [21]. Although the drugs used to treat RILI have been increasing in recent years, the complications caused by treatment are also inevitable [1,22]. Therefore, it is essential to seek better treatment for radiation lung injury.

Hydrogen is a new type of antioxidant. Many current studies have confirmed that the intake of hydrogen molecules through various ways can clear powerful oxygen free radicals, significantly inhibit inflammation, and reduce tissue and organ damage by reducing pro-

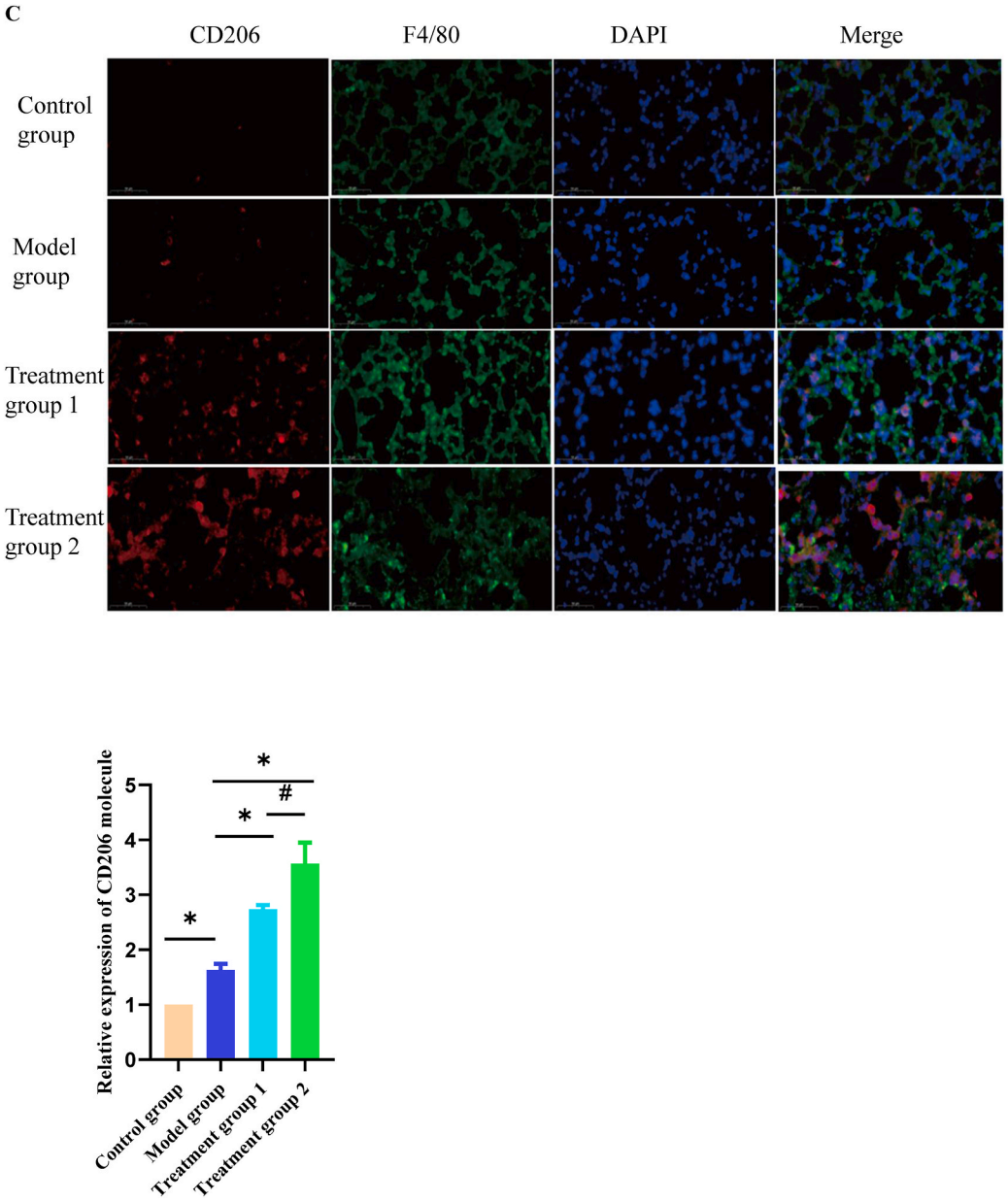

Fig. 2. (*continued*).

inflammatory cytokines [23–25]. Molecular hydrogen significantly inhibits NF-κB activation to reduce inflammatory responses [26,27]. It has been reported that hydrogen plays a specific therapeutic role in RILI [28], and hydrogen therapy has a protective effect on acute and advanced radiation-induced lung injury in vivo. But the exact mechanism still needs to be clarified. Therefore, it is urgent to study the particular therapeutic agent of hydrogen in RILI and find an effective hydrogen therapy for RILI.

Macrophages play an essential role in the body's immune defence. Macrophages can differentiate into specific functional phenotypes, and it is generally accepted that the M1 subtype is pro-inflammatory and is also known as pro-inflammatory macrophage.M1 subtype macrophages can kill pathogens and present their antigens to T lymphocytes to initiate an adaptive response. They produce high levels of pro-inflammatory cytokines such as TNF-α, IL-6, etc. The activation of the transcription factor NF-κB and nuclear translocation mainly controls the expression of these pro-inflammatory cytokines [17,29,30]. CD86 molecules can be expressed on the surface of M1 subtype macrophages. The M2 subtype is anti-inflammatory and is also known as anti-inflammatory macrophages, which express high levels of the mannose receptor (CD206) [29,30]. The M2 macrophage subtype is induced by immune cells' secretion of IL-4, IL-10 or IL-13. The M2 subtype of The M2 subtype of macrophages can induce the receptor IL-1R as well as IL-1R antagonists and produce pro-fibrotic factors such as transforming growth factor beta (TGF-β) and insulin-like growth factor 1

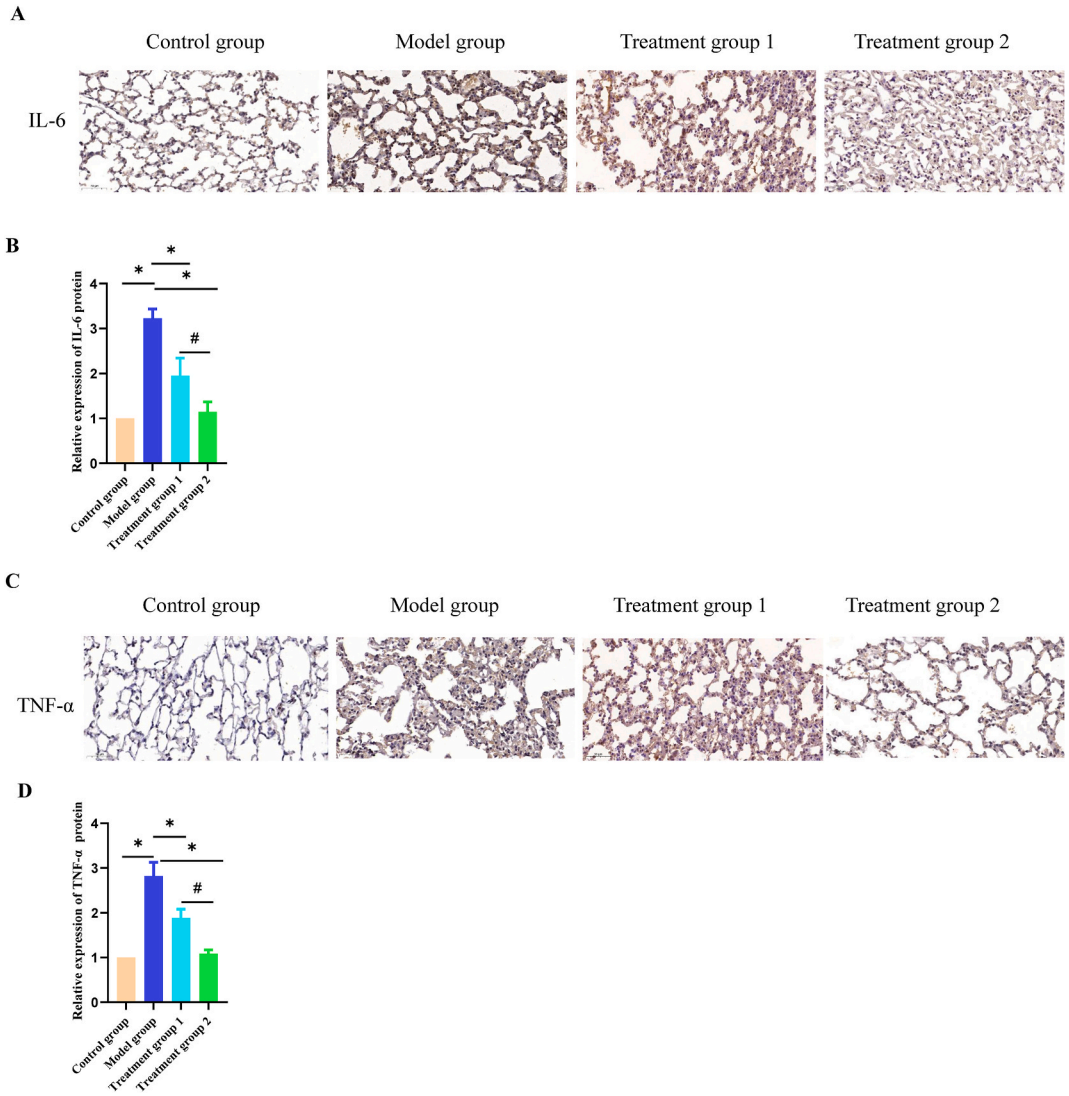

Fig. 3. Hydrogen therapy can significantly inhibit the inflammatory response in radiation-induced lung injury. **A:** The inflammatory cytokines IL-6 in the lung tissue were detected by immunohistochemistry. scale bar, 200 μm. **B:** Histogram of the expression levels of cytokines IL-6 in lung tissue by immunohistochemistry. Data are expressed as mean ± SD, n = 3.*Compared with the model group, $P < 0.05$. #Compared with the treatment group1, $P < 0.05$. **C:** The inflammatory cytokines TNF-a in the lung tissue were detected by immunohistochemistry. scale bar, 200 μm. **D:** Histogram of the expression levels of cytokines TNF-a in lung tissue by immunohistochemistry. Data are expressed as mean ± SD, n = 3.*Compared with the model group, $P < 0.05$. #Compared with the treatment group1, $P < 0.05$. **E:** The inflammatory cytokines IL-10 in the lung tissue were detected by immunohistochemistry. scale bar, 200 μm. **F:** Histogram of the expression levels of cytokines IL-10 in lung tissue by immunohistochemistry. Data are expressed as mean ± SD, n = 3.*Compared with the model group, $P < 0.05$. #Compared with the treatment group1, $P < 0.05$.

(IGF-1), which actively suppress inflammation and promote repair [17,29].When the body is exposed to ionizing radiation in the early stage, macrophages will be polarized toward the M1 subtype, generating inflammatory storms to promote the progression of radiation pneumonia [31]. In the middle and late stages of RILI, macrophages will be polarized towards the M2 type, and M2 subtype macrophages will promote the regression of inflammation and phagocytose apoptotic cells. An NF-κB signaling pathway is a classical anti-inflammatory pathway in which NF-κB, as a nuclear transcription factor, can induce the expression of inflammatory factors in immune cells and is an essential driving factor for macrophages to exert pro-inflammatory function, which promotes the polarization of macrophages towards M1 subtype [32]. It has been documented that inhibition or activation of the NF-κB signaling pathway can significantly affect the polarization state of macrophages [33,34].

The modelling method of radiation lung injury used in this study is based on the previously published literature of our research group.In the preliminary experiments of our group, C57BL/6J mice were used as irradiation carriers, and different irradiation doses of 0Gy, 8Gy, 12Gy, 16Gy and 20Gy were used to establish a mouse model of RILI, and mice were dissected 5w, 6w and 7w after

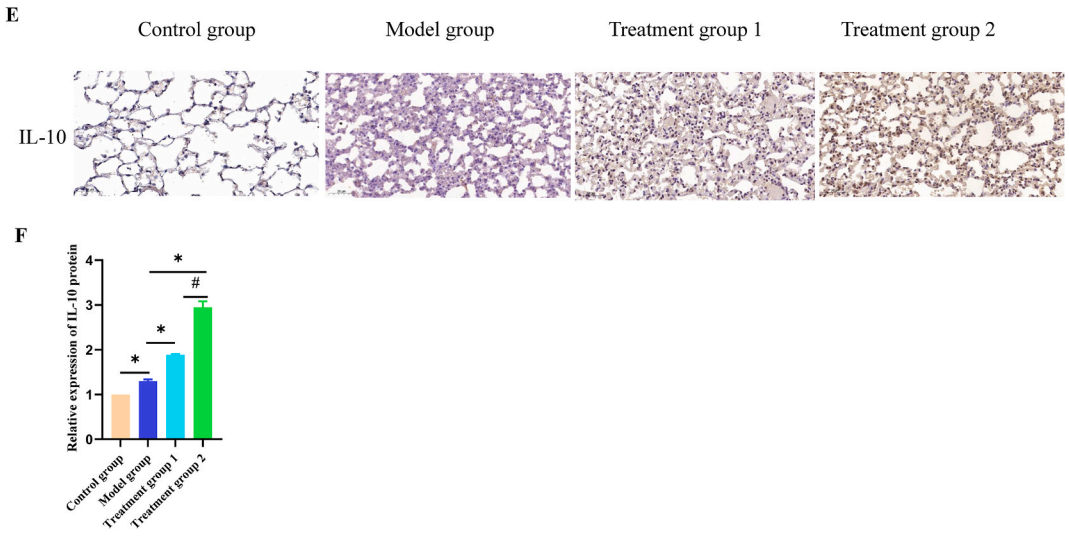

Fig. 3. (*continued*).

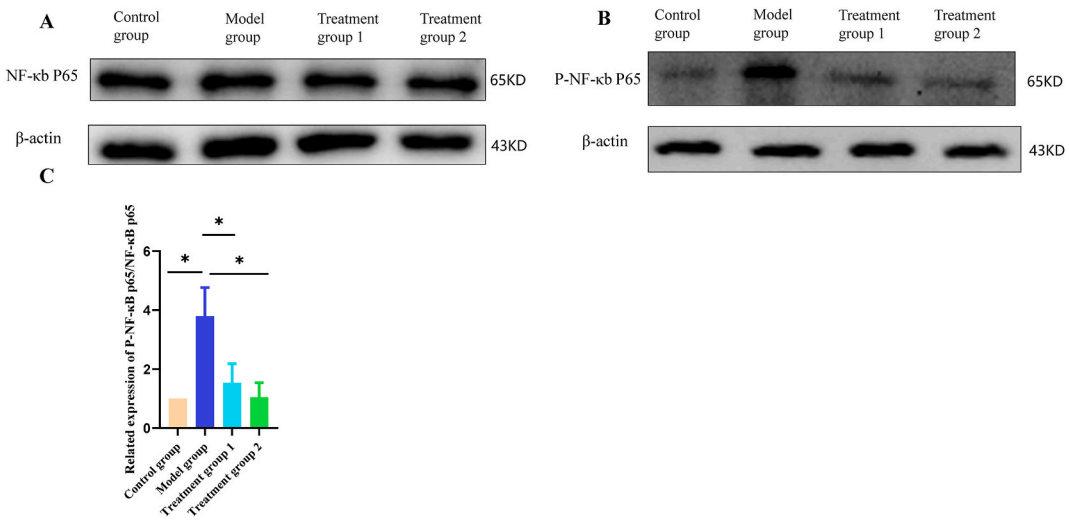

Fig. 4. Hydrogen therapy can significantly inhibit the NF-κB signaling pathway of inflammatory response.**A-B:** Images of NF-κB p65 and P–NF-κB 65 proteins detected by western blotting.**C:** Histogram of the Western blot grey values ratio of P–NF-κB p65 to NF-κB p65 proteins. Data are expressed as mean ± SD, n = 3.*Compared with the model group, $P < 0.05$.

irradiation, respectively. Based on the pathological changes in the lung tissue, we finally used an irradiation dose of 20 Gy to establish a mouse model of RILI and dissected the mice 5 weeks after irradiation [14]. Therefore,In this study, 6 MV X-ray was used to perform single chest irradiation on mice with a dose of 20Gy. Compared with the standard control group, the RILI model of mice was successfully established through edema and thickening of the alveolar septum in lung tissue, vascular dilation and congestion, and inflammatory cell infiltration in the model group [4]. Hydrogen gas is an effective antioxidant and can penetrate the blood-brain barrier through gaseous diffusion. Hydrogen gas is safe to use at concentrations between 2 and 5%, and inhalation of 3–4% H_2 gas does not cause adverse effects [35,36]. Studies have confirmed that 3.3 % hydrogen inhalation can improve and reduce oxidative stress-related endothelial cell damage after subarachnoid haemorrhage in rats and that 3.2 % hydrogen inhalation for 6 h per day for 21d can suppress bleomycin-induced decline in respiratory physiology and increase in alveolar fibrosis [37,38].4 % hydrogen inhalation is generally administered for 10 days [39]. Therefore, the present study used 4 % hydrogen inhalation, reducing the duration to 4h per day, with a 2-week and 5-week cycle, respectively.The model group was treated with hydrogen inhalation, and lung function changes were detected by lung function. The pathological changes in lung tissue were observed by HE staining. Macrophage polarization was observed by immunofluorescence. The expression of inflammatory factors IL-6, TNF-α and IL-10 in lung tissues was detected by immunohistochemistry. We verified that the lung lesions in the model group were significantly reduced after hydrogen therapy. The results of immunofluorescence and immunohistochemistry showed that the expression of M1 subtype macrophages in the model group

was up-regulated, and the major inflammatory cytokines IL-6 and TNF-α were produced. In the treatment group, the expression of M1 subtype macrophages was significantly down-regulated. In contrast, the expression of M2 subtype macrophages was up-regulated, the inflammatory cytokines IL-6 and TNF-α were significantly reduced, and the expression of the anti-inflammatory factor IL-10 was elevated.

Therefore, hydrogen therapy promoted the polarization of macrophages to the M2 subtype and alleviated the inflammatory response of radiation lung injury. To further investigate the protective effects of hydrogen on macrophages and the mechanisms that promote macrophage polarization, we used protein western blotting to detect the expression of inflammatory response-related signalling pathways in lung tissue proteins. Due to the presence of tissue proteins that are complex and depleting to extract, we only validated NF-κB p65 and P–NF-κB p65 protein expression for the available tissue proteins. There was a significant increase in P–NF-κB p65/NF-κB p65 in the model group compared with the control group. Compared with the model group, P–NF-κB p65/NF-κB p65 was significantly reduced in the hydrogen treatment group. Hydrogen therapy can dramatically inhibit the activation of the NF-κB signaling pathway. This experiment used two treatment cycles of 2 weeks and five weeks. Although both treatment cycles could achieve the effect of alleviating lung injury, the impact was more evident after five weeks of treatment.

The mechanism of hydrogen inhalation to inhibit inflammation is initially explored in this paper, but most of the current studies remain in the aspect of animal experiments, with fewer clinical trial studies. The study confirms that long-term hydrogen inhalation is safe for healthy people [40,41]. However, the concentration and duration of hydrogen inhalation affect the therapeutic effect [42–44]. Low H2 concentrations can be used to treat inflammation locally in the eye and in the ear and nose [45], whereas high inhalation concentrations do not necessarily improve therapeutic efficacy [46,47]. The signalling pathways involved in the treatment of radiological lung injury are complex, and each pathway interacts with each other, and the specific mechanisms need to be sorted out. Therefore, future studies need to further explore the mechanism of hydrogen inhalation in the treatment of radiological lung injury, conduct more extensive clinical studies to verify its safety and efficacy, and provide more evidence for the development of new anti-inflammatory drugs based on hydrogen inhalation in the future.The limitations of this study are that the hydrogen-regulated NF-κB signalling pathway has not been fully validated, and the specific mechanisms of its induction have not been thoroughly investigated.

5. Conclusion

In conclusion, the data in this study suggest that 4 % hydrogen inhalation for 4 h a day for a sustained period has a specific therapeutic effect on radiological lung injury, and the effect is more pronounced after 5 weeks. We can preliminarily infer that hydrogen can promote macrophage polarization from M1 to M2 subtypes by inhibiting the NF-κB signalling pathway, thereby reducing the inflammatory response to radiation lung injury.

Data availability

Data will be made available on request.

Ethics statement

All animal experiments were approved by the Experimental Animal Ethics Committee of Shandong First Medical University (W202311160312). All methods were performed in accordance with the relevant guidelines and regulations.

Funding sources

Natural Science Foundation of Shandong Province, No.ZR2020QH208; Health Science and Technology Development Program of Shandong Province(202101041037); Innovation and Entrepreneurship Training Program of Shandong First Medical University (2022104391744).

CRediT authorship contribution statement

Xue Gao: Formal analysis, Data curation, Conceptualization. **Shiying Niu:** Investigation. **Lulu Li:** Resources. **Xiaoyue Zhang:** Supervision. **Xuetao Cao:** Software. **Xinhui Zhang:** Methodology. **Wentao Pan:** Data curation. **Meili Sun:** Supervision. **Guoli Zhao:** Project administration. **Xuezhen Zheng:** Software. **Guohua Song:** Conceptualization. **Yueying Zhang:** Conceptualization.

Declaration of competing interest

The authors declare that they have no known competing financial interests or personal relationships that could have appeared to influence the work reported in this paper.

Acknowledgements

The authors thank the participants who participated in this study.

Appendix A. Supplementary data

Supplementary data to this article can be found online at https://doi.org/10.1016/j.heliyon.2024.e30902.

References

[1] A.N. Hanania, W. Mainwaring, Y.T. Ghebre, N.A. Hanania, M. Ludwig, Radiation-induced lung injury: assessment and management, Chest 156 (1) (2019) 150–162.
[2] L. Giuranno, J. Ient, D. De Ruysscher, M.A. Vooijs, Radiation-induced lung injury (RILI), Front. Oncol. 9 (2019) 877.
[3] Z. Chen, Z. Wu, W. Ning, Advances in molecular mechanisms and treatment of radiation-induced pulmonary fibrosis, Transl. Oncol. 12 (1) (2019) 162–169.
[4] S. Niu, Y. Zhang, C. Cong, Z. Wu, Z. Wang, M. Sun, C. Yao, Y. Zhang, Comparative study of radiation-induced lung injury model in two strains of mice, Health Phys. 122 (5) (2022) 579–585.
[5] J. Li, R. Wang, W. Shi, X. Chen, J. Yi, X. Yang, S. Jin, Epigenetic regulation in radiation-induced pulmonary fibrosis, Int. J. Radiat. Biol. 99 (3) (2023) 384–395.
[6] M. Arroyo-Hernández, F. Maldonado, F. Lozano-Ruiz, W. Muñoz-Montaño, M. Nuñez-Baez, O. Arrieta, Radiation-induced lung injury: current evidence, BMC Pulm. Med. 21 (1) (2021) 9.
[7] M.J. McCarty, P. Lillis, S.J. Vukelja, Azathioprine as a steroid-sparing agent in radiation pneumonitis, Chest 109 (5) (1996) 1397–1400.
[8] T. Muraoka, S. Bandoh, J. Fujita, A. Horiike, T. Ishii, Y. Tojo, A. Kubo, T. Ishida, Corticosteroid refractory radiation pneumonitis that remarkably responded to cyclosporin A, Intern. Med. 41 (9) (2002) 730–733.
[9] J. Li, G. Huang, J. Wang, S. Wang, Y. Yu, Hydrogen regulates ulcerative colitis by affecting the intestinal redox environment, J. Inflamm. Res. 17 (2024) 933–945.
[10] Y. Yu, Y. Yang, Y. Bian, Y. Li, L. Liu, H. Zhang, K. Xie, G. Wang, Y. Yu, Hydrogen gas protects against intestinal injury in wild type but not NRF2 knockout mice with severe sepsis by regulating HO-1 and HMGB1 release, Shock 48 (3) (2017) 364–370.
[11] N. Zhao, R. Sun, Y. Cui, Y. Song, W. Ma, Y. Li, J. Liang, G. Wang, Y. Yu, J. Han, et al., High concentration hydrogen mitigates sepsis-induced acute lung injury in mice by alleviating mitochondrial fission and dysfunction, J. Pers. Med. 13 (2) (2023).
[12] K. Zhou, M. Liu, Y. Wang, H. Liu, B. Manor, D. Bao, L. Zhang, J. Zhou, Effects of molecular hydrogen supplementation on fatigue and aerobic capacity in healthy adults: a systematic review and meta-analysis, Front. Nutr. 10 (2023) 1094767.
[13] B. Liu, Y. Xie, J. Chen, J. Xue, X. Zhang, M. Zhao, X. Jia, Y. Wang, S. Qin, Protective effect of molecular hydrogen following different routes of administration on D-galactose-induced aging mice, J. Inflamm. Res. 14 (2021) 5541–5550.
[14] S. Niu, Y. Zhang, C. Cong, Z. Wu, Z. Wang, M. Sun, C. Yao, Y. Zhang, Comparative study of radiation-induced lung injury model in two strains of mice, Health Phys. 122 (5) (2022) 579–585.
[15] C. Cong, S. Niu, Y. Jiang, X. Zhang, W. Jing, Y. Zheng, X. Zhang, G. Su, Y. Zhang, M. Sun, Renin-angiotensin system inhibitors mitigate radiation pneumonitis by activating ACE2-angiotensin-(1-7) axis via NF-κB/MAPK pathway, Sci. Rep. 13 (1) (2023) 8324.
[16] S. Gordon, A. Plüddemann, F. Martinez Estrada, Macrophage heterogeneity in tissues: phenotypic diversity and functions, Immunol. Rev. 262 (1) (2014) 36–55.
[17] A. Mantovani, A. Sica, S. Sozzani, P. Allavena, A. Vecchi, M. Locati, The chemokine system in diverse forms of macrophage activation and polarization, Trends Immunol. 25 (12) (2004) 677–686.
[18] Y. Yan, J. Fu, R.O. Kowalchuk, C.M. Wright, R. Zhang, X. Li, Y. Xu, Exploration of radiation-induced lung injury, from mechanism to treatment: a narrative review, Transl. Lung Cancer Res. 11 (2) (2022) 307–322.
[19] Y. Yan, L. Wu, X. Li, L. Zhao, Y. Xu, Immunomodulatory role of azithromycin: potential applications to radiation-induced lung injury, Front. Oncol. 13 (2023) 966060.
[20] S. Shrishrimal, E.A. Kosmacek, R.E. Oberley-Deegan, Reactive oxygen species drive epigenetic changes in radiation-induced fibrosis, Oxid. Med. Cell. Longev. 2019 (2019) 4278658.
[21] T.A. Beach, J.N. Finkelstein, P.Y. Chang, Epithelial responses in radiation-induced lung injury (RILI) allow chronic inflammation and fibrogenesis, Radiat. Res. 199 (5) (2023) 439–451.
[22] H.-J. Ying, M. Fang, M. Chen, Progress in the mechanism of radiation-induced lung injury, Chinese Med J-Peking 134 (2) (2020) 161–163.
[23] J.S. Dumbuya, S. Li, L. Liang, Y. Chen, J. Du, Q. Zeng, Effects of hydrogen-rich saline in neuroinflammation and mitochondrial dysfunction in rat model of sepsis-associated encephalopathy, J. Transl. Med. 20 (1) (2022) 546.
[24] M. Yu, C. Qin, P. Li, Y. Zhang, Y. Wang, J. Zhang, D. Li, H. Wang, Y. Lu, K. Xie, et al., Hydrogen gas alleviates sepsis-induced neuroinflammation and cognitive impairment through regulation of DNMT1 and DNMT3a-mediated BDNF promoter IV methylation in mice, Int. Immunopharmacol. 95 (2021) 107583.
[25] S. Roy, K.E. Salerno, D.E. Citrin, Biology of radiation-induced lung injury, Semin. Radiat. Oncol. 31 (2) (2021) 155–161.
[26] C. Wang, J. Li, Q. Liu, R. Yang, J.H. Zhang, Y.-P. Cao, X.-J. Sun, Hydrogen-rich saline reduces oxidative stress and inflammation by inhibit of JNK and NF-κB activation in a rat model of amyloid-beta-induced Alzheimer's disease, Neurosci. Lett. 491 (2) (2011) 127–132.
[27] C.-B. Zhang, Y.-C. Tang, X.-J. Xu, S.-X. Guo, H.-Z. Wang, Hydrogen gas inhalation protects against liver ischemia/reperfusion injury by activating the NF-κB signaling pathway, Exp. Ther. Med. 9 (6) (2015) 2114–2120.
[28] Y. Terasaki, I. Ohsawa, M. Terasaki, M. Takahashi, S. Kunugi, D.D. Kang, H. Urushiyama, S. Amenomori, M. Kaneko-Togashi, N. Kuwahara, et al., Hydrogen therapy attenuates irradiation-induced lung damage by reducing oxidative stress, Am. J. Physiol. Lung C 301 (4) (2011) L415–L426.
[29] A. Viola, F. Munari, R. Sánchez-Rodríguez, T. Scolaro, A. Castegna, The metabolic signature of macrophage responses, Front. Immunol. 10 (2019) 1462.
[30] E. Apeku, M.M. Tantuoyir, R. Zheng, N. Tanye, Exploring the polarization of M1 and M2 macrophages in the context of skin diseases, Mol. Biol. Rep. 51 (1) (2024) 269.
[31] R. Yahyapour, D. Shabeeb, M. Cheki, A.E. Musa, B. Farhood, A. Rezaeyan, P. Amini, H. Fallah, M. Najafi, Radiation protection and mitigation by natural antioxidants and flavonoids: implications to radiotherapy and radiation disasters, Curr. Mol. Pharmacol. 11 (4) (2018) 285–304.
[32] K.S. Alharbi, N.K. Fuloria, S. Fuloria, S.B. Rahman, W.H. Al-Malki, M.A. Javed Shaikh, L. Thangavelu, S.K. Singh, V.S. Rama Raju Allam, N.K. Jha, et al., Nuclear factor-kappa B and its role in inflammatory lung disease, Chem. Biol. Interact. 345 (2021) 109568.
[33] Q. Zhang, Z. Mao, J. Sun, NF-κB inhibitor, BAY11-7082, suppresses M2 tumor-associated macrophage induced EMT potential via miR-30a/NF-κB/Snail signaling in bladder cancer cells, Gene 710 (2019) 91–97.
[34] T. Li, L. Li, R. Peng, H. Hao, H. Zhang, Y. Gao, C. Wang, F. Li, X. Liu, F. Chen, et al., Abrocitinib attenuates microglia-mediated neuroinflammation after traumatic brain injury via inhibiting the JAK1/STAT1/NF-κB pathway, Cells 11 (22) (2022).
[35] Y. Zhan, C. Chen, H. Suzuki, Q. Hu, X. Zhi, J.H. Zhang, Hydrogen gas ameliorates oxidative stress in early brain injury after subarachnoid hemorrhage in rats, Crit. Care Med. 40 (4) (2012) 1291–1296.
[36] S. Ohta, Molecular hydrogen as a preventive and therapeutic medical gas: initiation, development and potential of hydrogen medicine, Pharmacol. Ther. 144 (1) (2014).
[37] K. Zhuang, Y.-C. Zuo, P. Sherchan, J.-K. Wang, X.-X. Yan, F. Liu, Hydrogen inhalation attenuates oxidative stress related endothelial cells injury after subarachnoid hemorrhage in rats, Front. Neurosci. 13 (2019) 1441.
[38] T. Aokage, M. Seya, T. Hirayama, T. Nojima, M. Iketani, M. Ishikawa, Y. Terasaki, A. Taniguchi, N. Miyahara, A. Nakao, et al., The effects of inhaling hydrogen gas on macrophage polarization, fibrosis, and lung function in mice with bleomycin-induced lung injury, BMC Pulm. Med. 21 (1) (2021) 339.

[39] B. Liu, Y. Xie, J. Chen, J. Xue, X. Zhang, M. Zhao, X. Jia, Y. Wang, S. Qin, Protective effect of molecular hydrogen following different routes of administration on D-galactose-induced aging mice, J. Inflamm. Res. 14 (2021) 5541–5550.
[40] A.R. Cole, F. Sperotto, J.A. DiNardo, S. Carlisle, M.J. Rivkin, L.A. Sleeper, J.N. Kheir, Safety of prolonged inhalation of hydrogen gas in air in healthy adults, Crit Care Explor 3 (10) (2021) e543.
[41] Y. Saitoh, Y. Harata, F. Mizuhashi, M. Nakajima, N. Miwa, Biological safety of neutral-pH hydrogen-enriched electrolyzed water upon mutagenicity, genotoxicity and subchronic oral toxicity, Toxicol. Ind. Health 26 (4) (2010) 203–216.
[42] I. Ohsawa, M. Ishikawa, K. Takahashi, M. Watanabe, K. Nishimaki, K. Yamagata, K.-I. Katsura, Y. Katayama, S. Asoh, S. Ohta, Hydrogen acts as a therapeutic antioxidant by selectively reducing cytotoxic oxygen radicals, Nat Med 13 (6) (2007) 688–694.
[43] M. Ito, M. Hirayama, K. Yamai, S. Goto, M. Ito, M. Ichihara, K. Ohno, Drinking hydrogen water and intermittent hydrogen gas exposure, but not lactulose or continuous hydrogen gas exposure, prevent 6-hydorxydopamine-induced Parkinson's disease in rats, Med. Gas Res. 2 (1) (2012) 15.
[44] Y. Terasaki, I. Ohsawa, M. Terasaki, M. Takahashi, S. Kunugi, K. Dedong, H. Urushiyama, S. Amenomori, M. Kaneko-Togashi, N. Kuwahara, et al., Hydrogen therapy attenuates irradiation-induced lung damage by reducing oxidative stress, Am. J. Physiol. Lung Cell Mol. Physiol. 301 (4) (2011) L415–L426.
[45] Y. Wu, M. Yuan, J. Song, X. Chen, H. Yang, Hydrogen gas from inflammation treatment to cancer therapy, ACS Nano 13 (8) (2019) 8505–8511.
[46] B. Liu, J. Xue, M. Zhang, M. Wang, T. Ma, M. Zhao, Q. Gu, S. Qin, Hydrogen inhalation alleviates nonalcoholic fatty liver disease in metabolic syndrome rats, Mol. Med. Rep. 22 (4) (2020) 2860–2868.
[47] X. Liu, C. Ma, X. Wang, W. Wang, Z. Li, X. Wang, P. Wang, W. Sun, B. Xue, Hydrogen coadministration slows the development of COPD-like lung disease in a cigarette smoke-induced rat model, Int. J. Chron. Obstruct. Pulmon. Dis. 12 (2017) 1309–1324.